Experimental comparison of the measurement results of two different silicon photomultipliers and organic scintillator to detect fast neutrons

Experimental comparison of the measurement results of two different silicon photomultipliers and organic scintillator to detect fast neutrons

A C Chergui[1], E V Popova[1], A A Stifutkin[1], O Dendene[1], A L Ilyin[1], S L Vinogradov[1,2] and O V Bychkova[1]

[1] National Research Nuclear University MEPhI (Moscow Engineering Physics Institute), Kashirskoe Shosse 31, Moscow, 115409, Russian Federation
[2] P.N. Lebedev Physical Institute of the Russian Academy of Sciences, Leninskiy Prospekt 53, Moscow, 119991, Russian Federation

E-mail: cherguicherif@hotmail.com

Abstract. We report on the study of experimental comparison between the results of two types of silicon photomultiplier (SiPM), to discriminate the signals from fast neutrons and gamma-rays by the digital charge pulse shape discrimination (PSD) method. This uses a total to partial charge ratio analysis. The signals are digitized by a high-speed digital oscilloscope LeCroy WR 620zi with a sample rate of 10 GS/s. This oscilloscope was used to acquire data, which were later processed offline in a specially developed software package written in LABVIEW. The tested detector part consisted from a stilbene crystal (3x3x6 mm^3 and 6x6x6 mm^3) optically coupled to a SiPM (KETEK 3x3 mm^2 and SensL 6x6 mm^2 respectively) as a photodetector. Measurements with a Cf-252 source were performed and a figure of merit (FOM) for discrimination between neutron and gamma-ray was calculated for each assembly. The resulting value of FOM for the KETEK 3x3 mm^2 SiPM and SensL 6x6 mm^2 SiPM was 1.6±0.03 and 1.76±0.05, respectively, the SensL assembly having a slightly better discrimination factor than KETEK one. The obtained results prove a good fast neutron detection performance of the SiPMs, which makes it possible to use these types of neutron detectors in the several fields of radiation protection applications and safety of nuclear facilities.

1. Introduction

Neutron detection and spectrometry are very important in various fields of research. The various fields include: nuclear industry, radiation protection, safeguards, protection of personnel in nuclear installations and the problem of controlling the spread of nuclear material. For many years, fission chambers and gas proportional counters like ^3He and BF_3 are widely in use for the detection and dosimetry of thermal neutrons. To detect fast neutrons, these detectors are surrounded by a decelerating material (moderator) such as polyethylene or water, which reduces the detection efficiency on the one hand, and increases its volume on the other. Among the disadvantages of this type of detector are, for example, the scarcity of the ^3He gas and its relatively high cost. In addition, the gas in the detector tube loses its pressure over time, which forces it to be calibrated for efficiency from time to time for a more accurate measurement. This type of detector is usually used as a neutron counter and cannot be used for real-time neutron spectrometry [1].

Some types of liquid and crystalline organic scintillators combined with a photoelectron multiplier are well suited for fast neutron spectrometry; however, the liquid organic scintillators are not suitable for many field applications due to potential leakage and fire hazards [2]. This type of detector is based on the principle of creating recoil protons in a scintillator, which induce a scintillation process on their trajectory. Organic scintillators are also sensitive to gamma radiation, which create recoil electrons via the Compton effect and photoelectric effect [3], such gamma-ray induced scintillations may present a background that limits the effective measurement of fast neutron flux.

Since these organic scintillators produce light flashes of different shape depending on the linear energy transfer (LET) of the ionizing particle passing through its volume, it is possible to separate neutron pulses from gamma quanta pulses. Such separation based on the pulse shape discrimination (PSD) technique, which is well established method used for separating neutron-induced signals from gamma-induced ones during measurements of mixed neutron and gamma fields. The PSD technique discriminates scintillations from high-energy electrons produced in collisions with gamma-rays from those caused by neutron-scattered recoil-nuclei (heavy charged particles) [4, 5].

The organic scintillator crystal stilbene ($C_{14}H_{12}$) is one of the best scintillators used for fast neutron detection. For many years stilbene crystals were applied for fast neutron detection in the neutron energy range from 500 keV to 20 MeV due to their good timing performance (<10 ns), detection efficiency, and excellent pulse shape discrimination properties in mixed neutrons and gamma radiation fields [6, 7].

A photoelectric multiplier (PMT) is traditionally used to amplify and convert a scintillation light pulse into an electrical signal that can be processed and stored. A PMT has high internal gain, fast response, and low noise. However, this device has also some disadvantages, such as sensitivity to magnetic and electric fields, a high operating voltage (1800 V) and large volume, resulting in limit on its scope of application in the field of radiation protection, nuclear security and problems of controlling the spread of nuclear material [8].

A light detector that eliminates these disadvantages and facilitates the use and extends the scope of neutron detection will be a good alternative to the traditional photoelectric multiplier.

The latest generations of SiPMs currently available have comparable and sometimes better characteristics than PMT tubes, such as insensitivity to magnetic and electric fields, strength, small size, high gain, high photon detection efficiency, low power consumption and operation with low electrical voltage (20-60 V) [9, 10]. That gives them a great opportunity to become a promising replacement for vacuum photomultipliers for various neutron detection applications. However, the SiPMs exhibit some characteristics that present a challenge for precise electronic readout. These include a longer single photon response duration and relatively higher noise contributions from dark pulses, after-pulsing [11].

The main goals of this work is to compare two SiPM sensors in terms of fast neutron detection performance and discrimination between neutrons and gamma rays by applying the method of PSD and a development of a specially software package written in LABVIEW for data analysis.

2. Experimental methodology

2.1. Experiment setup

The detector part consisted of a stilbene crystal 3x3x6 mm^3 and 6x6x6 mm^3 that was carefully wrapped with Teflon tape (figure 1a) to prevent leakage of scintillation light and improve light collection. Those stilbene crystals were mounted respectively onto a SiPM manufactured by KETEK, model number PM3325 WB (figure 1b), that has an active area of 3x3 mm^2 [12] and SiPM manufactured by SensL, model number MicroFC-60035-SMT (figure 1c), which has an active area of 6x6 mm^2 [13]. The main characteristics of the studied SiPMs are reflected in table 1. The optical silicon grease (BC-630, Saint-Gobain) was used to achieve optimal photon

transfer [14]. Each SiPM was installed on an evaluation board equipped with two connectors – SiPM power and signal. The detector assemblies (the stilbene scintillator and SiPM) were placed in a light-tight box painted black inside to minimize stray light. The Keithley 2400 sourcemeter was used to supply the SiPMs with a bias voltage; this sourcemeter works as a very accurate voltage or current source simultaneously providing precise output voltage and current measurements [15]. The detector assembly was tested experimentally using ^{252}Cf fission source, providing mixed neutron and gamma radiation with an intensity of 10^4 neutrons/s, this source is normally placed on the top of a 1.5 meter long cylindrical rod. During measurements the source was moved manually to the edge of the detector assembly box and placed about 20 cm from the edge. The output signals from the SiPM evaluation board were digitized directly without any analog shaping or external amplifier.

A high-speed digital oscilloscope connected to the evaluation board via 50 Ω coaxial cable was used to acquire data. All measurements were carried on at a constant room temperature. Figure 2 shows a schematic diagram of the experimental setup for the radiation measurements.

Table 1. Some characteristics of studied sensors.

Characteristics / Sensor(SiPM)	PM3325 WB	MicroFC-60035-SMT
Manufacturer	KETEK	SensL
Package	PM	SMT
Maximum sensitivity wavelength (nm)	430	420
Photosensitive surface size (mm)	3	6
Pixel pitch (µm)	25	35
Gain	10^6	3×10^6
Photon detection efficiency (PDE)	38%	35%
Supply voltage (V)	28.5	27.5
Recommended operating temperature range	-40°C to +60°C	-40°C to +85°C

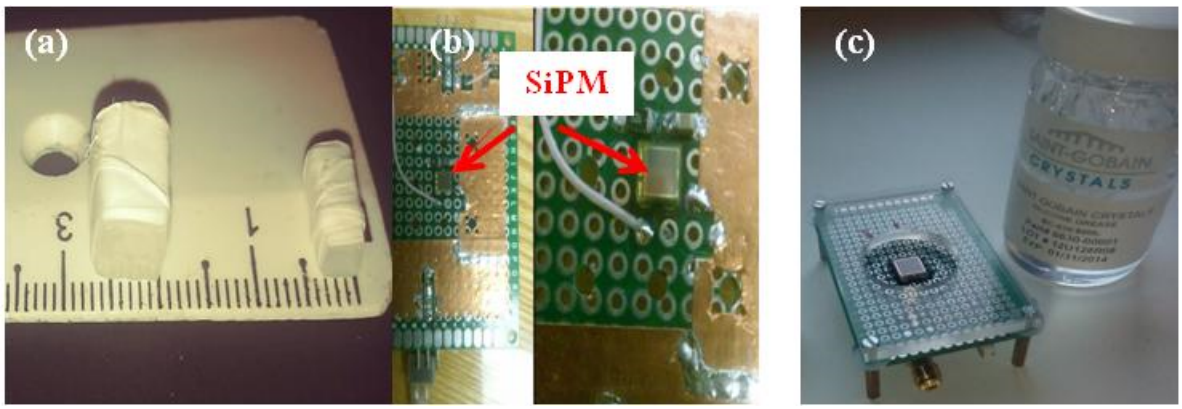

Figure 1. Photo of the detector assembly used in this experiment: (a) – the stilbene crystals (3x3x6 mm^3 and 6x6x6 mm^3) wrapped with Teflon tape, (b) – PM3325 WB, (c) – MicroFC-60035-SMT.

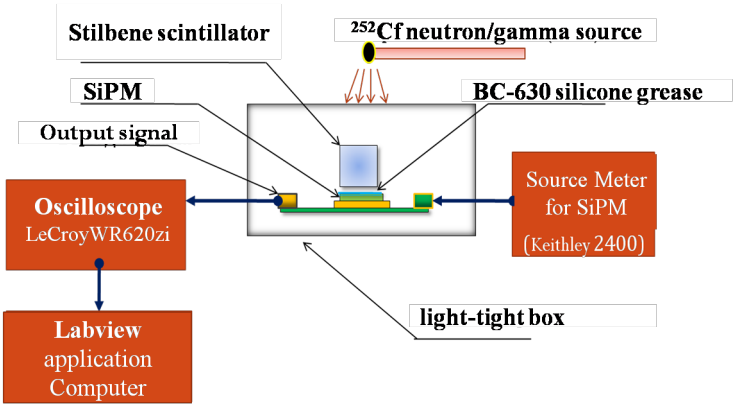

Figure 2. Diagram of the experimental setup.

2.2. Data processing software

The sensor signals were digitized by a high-speed digital oscilloscope LeCroyWR 620zi with a sample rate of 10 GS/s, the acquired waveforms stored and later processed offline in a specially developed software package written in LABVIEW. Screenshots of the software shown in figure 3.

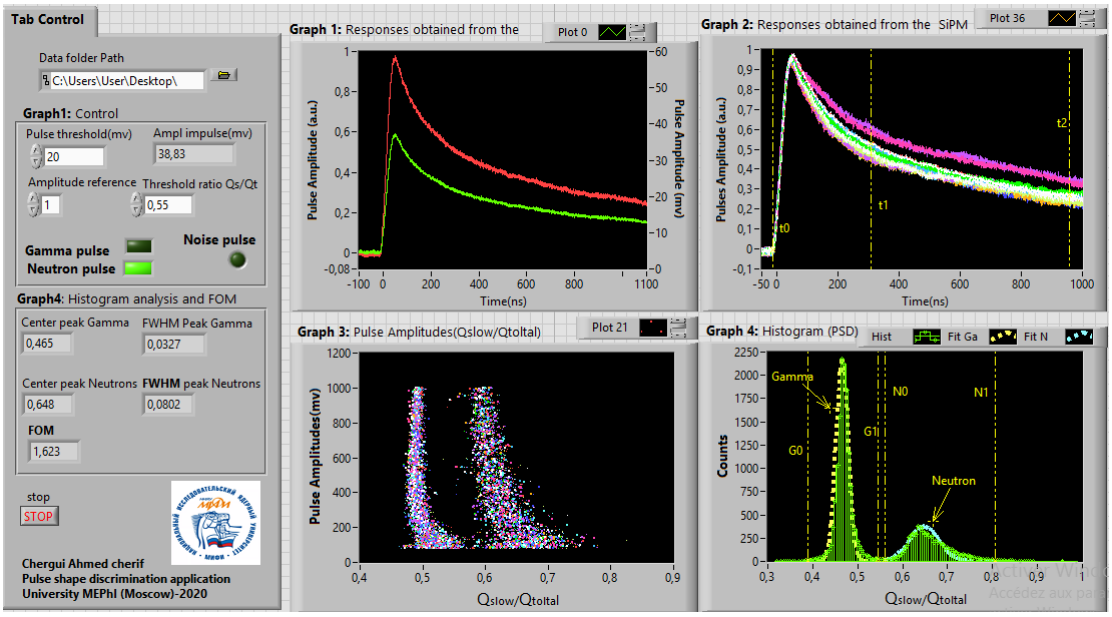

Figure 3. Developed software for data processing written in LABVIEW.

This program provides several parameters for configuring and selecting the type and properties of the input file. The program also allows discarding of the distorted pulses and selecting a method for separating neutron pulses from gamma-ray pulses. Dark noise was in the order of 21 mV, which caused fluctuation in baseline and posed a challenge on PSD, so the program provides a threshold of 21.5 mV for discarding undesirable pulses.

Each pulse was normalized and accumulated to determine the optimal time intervals when analyzing and comparing slow and fast components. All charts and results presented in these

papers have been extracted from this software.

3. Results

The typical pulse shape measured with this setup presented in figure 4, which shows the shapes of the pulses of a recoil proton (neutron) recorded by the different sensors (MicroFC-60035-SMT and PM3325 WB) in combination with the stilbene crystal. It is clear that pulse's rise and fall constants are defined by the SiPM time properties, so different time intervals to calculate total and tail (slow component) charges were selected for different SiPM.

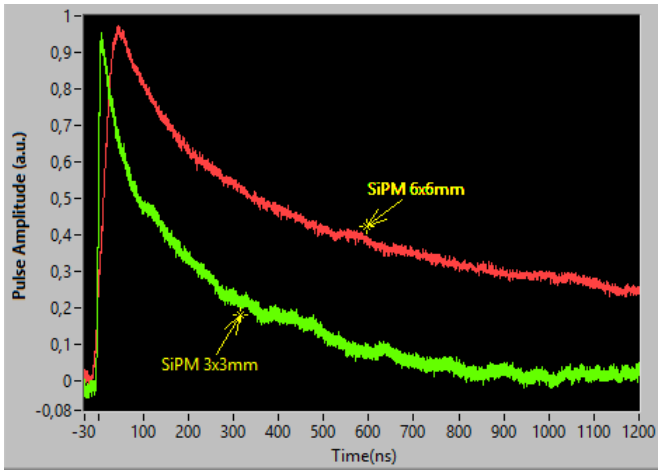

Figure 4. Uniformity of responses of the sensors used: MicroFC-60035-SMT (SensL 6x6 mm^2) and PM3325 WB (KETEK 3x3 mm^2).

Figure 5 shows the recorded pulse shapes of the source radiations by the two studied sensors. There is an important information that can be observed in this figure – the duration of the pulses, extending to about 1600 ns for the sensor MicroFC-60035-SMT and about 700 ns for the sensor PM3325 WB, strongly defined by SiPMs time properties, such as a single cell recovery time, which, in turn, depends on a detector electrical layout [16, 17]. Generally speaking, smaller SiPMs with smaller cells have faster response, resulting in a higher maximum count rate.

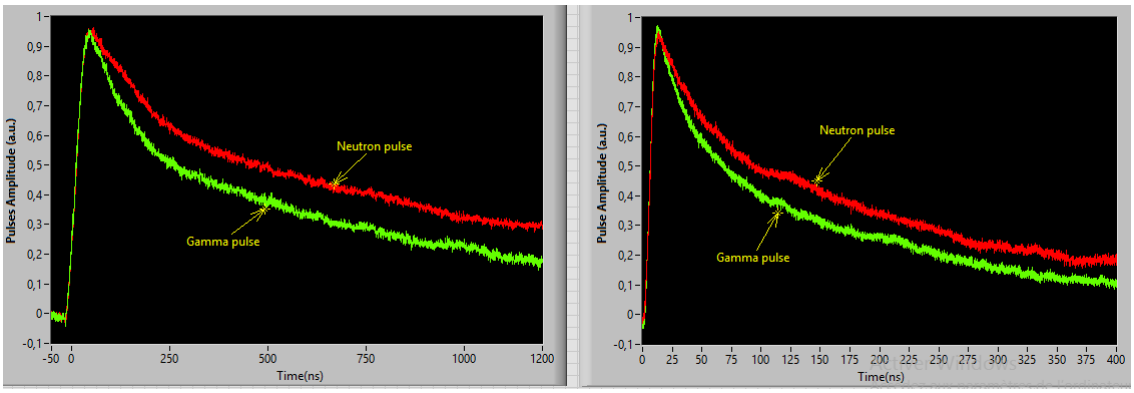

Figure 5. Comparison between a fast neutron pulse and a gamma-ray pulses measured using stilbene coupled to a MicroFC-60035-SMT (left) and PM3325 WB (right).

The principle of the PSD method based on the difference in the ratio of fast and slow components of the scintillation flash. It is possible to observe various shapes of flash illumination in organic scintillators when they register charged particles that create different ionization densities. Figure 6 shows some pulses recorded by the sensor MicroFC-60035-SMT, where pulses are normalized and adjusted to the same time reference and presented in the same figure. From figure 6 the difference of neutron pulses to those of gamma rays by the combination stilbene-MicroFC-60035-SMT is largely evident. The figure 6 also shows the limits of the intervals (time parameters) for digital integration of the recorded waveforms for the comparison of the slow part charges with the total charges.

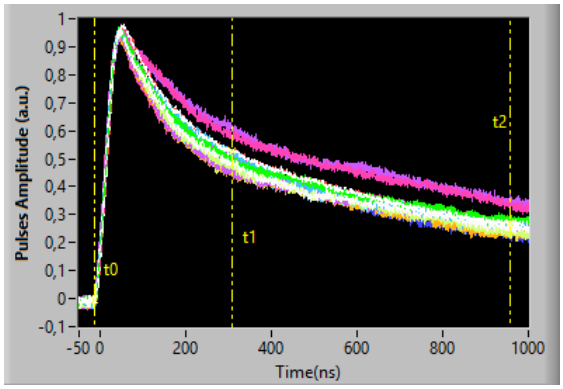

Figure 6. Comparison between fast neutron pulses and gamma ray pulses recorded by the MicroFC-60035-SMT SiPM.

The following equation describes the use of the time intervals shown in figure 6 for the determination of separation ratios Q_{slow}/Q_{total} of pulse shape discrimination method.

$$\frac{Q_{slow}}{Q_{total}} = \frac{\int_{t1}^{t2} V(t)\mathrm{d}t}{\int_{t0}^{t2} V(t)\mathrm{d}t} \tag{1}$$

Where: t is the time and $V(t)$ is the pulse waveform function.

Figures 7a and 7b show the pulse discrimination distributions recorded by the two sensors PM3325-WB and MicroFC-60035-SMT respectively. Each point on each graph presents a pulse defined by its own ratio Q_{slow}/Q_{total} and its amplitude in mV. All pulses of neutrons and gamma rays with amplitude greater than 21.5 mV are successfully discriminated and the two figures show that signatures of the two radiations are well separated.

The histograms in figures 8a and 8b represent the number of pulses recorded by the two studied sensors as a function of the Q_{slow}/Q_{total} ratio. The distribution of each radiation (neutrons or gamma radiation) is shown separately in the two figures. In order to evaluate the quality of discrimination each distribution is presented by a close Gaussian distribution as shown in the two figures. The following equation determines the figure of merit (FOM) for each sensor.

$$FOM = \frac{M}{FWHM_G + FWHM_N} \tag{2}$$

Where: FOM – figure of merit; M – the distance between the centers of the Gaussian

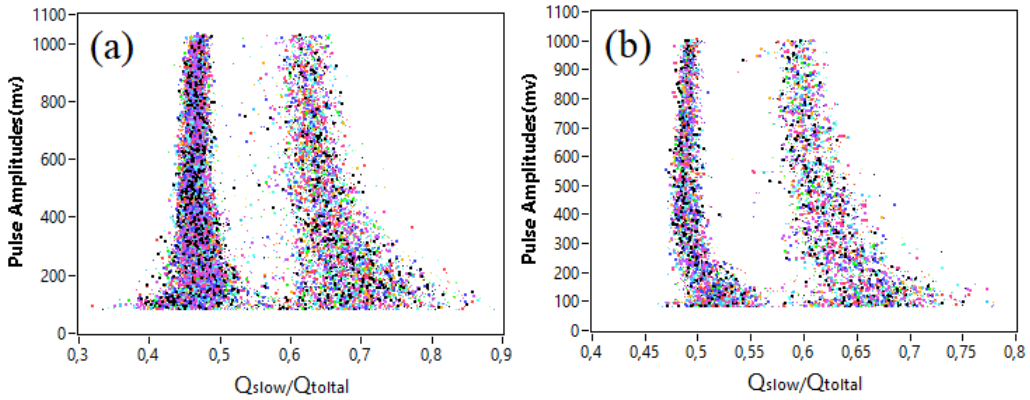

Figure 7. Tail to total ratio versus pulse height for pulses produced by a stilbene crystal coupled to (a) KETEK 3x3 mm^2 (b) SensL 6x6 mm^2. Cf-252 source.

distributions of neutrons and gamma rays signals, $FWHM_G$ and $FWHM_N$ – full width at half maximum of gamma-ray and neutron distributions, respectively.

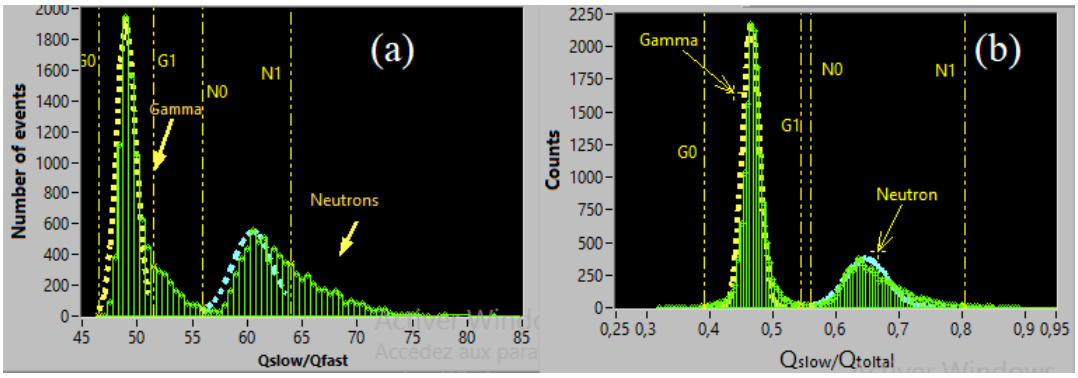

Figure 8. Histogram of the tail to total integral ratio from a measurement of Cf-252 using a stilbene crystal coupled to (a) SensL 6x6 mm^2 (b) KETEK 3x3 mm^2.

The calculated value of FOM for the sensors PM3325-WB and MicroFC-60035-SMT – 1.60±0.03 and 1.76 ±0.05 respectively.

4. Discussion

Considering our results – the FOM values pointed above – we have to turn to other studies on the neutron-gamma discrimination with the stilbene crystals. Many of them are based on the charge comparison method utilizing difference in the Q_{slow}/Q_{total} ratio. The method was established in the 1960s and is widely recognized now as the most simple, reliable, and efficient one for that case [4, 18]. Similar PSD FOM values of 1.7 at 300 keV have been reported for both the charge comparison and constant fraction discriminator methods with PMTs [19, 20]. High photon detection efficiency of SiPM allows to get the FOM of 2.13 at 200 keV for the same MicroFC-60035 SiPM and the single 6x6x6 mm^3 stilbene crystal. However, the whole experimental setup in the studies could hardly be exactly the same as its optical, photoelectric, electronic, and processing features are different even with the same scintillator and photodetector, we need

some solid grounds to evaluate the FOM performance and be able to compare experiments with each other as well as with theoretical limits.

Cramer-Rao lower bound (CRLB) seems to be an appropriate technique to evaluate an absolute limit of the FOM estimation. As an initial attempt, let us consider a simplified model of the particle detection: a single-exponential pulse shape of decay time T_{decay} (T_n and T_g for neutrons and gammas correspondingly). Probability density function of a single scintillation photon detection event time in this case is

$$f(t, T_{decay}) = \frac{1}{T_{decay}} \exp\left(-\frac{1}{T_{decay}}\right) \tag{3}$$

Therefore, the decay time is a single parameter to be estimated by any PSD algorithm as soon as the particles should be discriminated at the same energy (the same number of detected photons or total charge).

The Fisher information integral for a decay time in a single photon detection process is

$$I(T_{decay}) = \int_0^\infty \left(\frac{\partial}{\partial T_{decay}} \log f(t, T_{decay})\right)^2 \times f(t, T_{decay}) \mathrm{d}t = \frac{1}{T_{decay}^2} \tag{4}$$

In case of detection of N_{det} scintillation photons (often specified in terms of photoelectrons for PMT or fired pixels for SiPM), the Fisher information integrals are summed up, and CRLB of lowest possible variance in any estimation of T_{decay} is defined as

$$Var_{CRLB}(T_{decay}, N_{det}) = \frac{1}{N_{det} \times I(T_{decay})} = \frac{T_{decay}^2}{N_{det}} \tag{5}$$

Therefore, corresponding $FWHM$ is

$$FWHM_{CRLB}(T_{decay}, N_{det}) \approx \frac{2.35 \times T_{decay}}{\sqrt{N_{det}}} \tag{6}$$

Applying this result to the FOM based on any estimation of T_{decay} for neutrons and gammas as T_n and T_g, we get

$$FOM_{CRLB}(T_n, T_g, N_{det}) = \frac{\sqrt{N_{det}}}{2.35} \times \frac{T_n - T_g}{T_n + T_g} \tag{7}$$

As clearly seen, for the best experimental setup with the same scintillator and photodetector, we need to maximize optical coupling and photon detection efficiency as well as the relative difference in transient dynamics of the scintillation processes by acquisition electronics.

In fact, scintillation processes in the stilbene are typically characterized by three decay times of a wide range (4.3 ns, 34.8 ns, and 332 ns as reported in [21]), but we expect that CRLB FOM estimation could be based on some effective decay times. For example, decay of the plots in figure 6 to 1/e level approximately defines $T_n \sim 900$ ns and $T_g \sim 600$ ns. If to estimate N_{det} in a very coarse way by stilbene light yield of 10700 ph/MeV [19] and efficiency of photon detections by SiPM of 30% then CRLB FOM based on decay times is found to be ~ 2.16 at 200 keV.

5. Conclusion

The comparison between the sensor SiPM3325 WB (KETEK 3x3 mm^2) and the sensor MicroFC-60035-SMT (SensL 6x6 mm^2) in term of capability of effective pulse shape discrimination has shown that the PDS FOM doesn't really depend on the size of the sensor SiPM. Both sensors showed good neutron-gamma-ray discrimination capabilities. The sensor SiPM3325-WB recorded mixed radiations with shorter pulses than the sensor MicroFC-60035-SMT which

gives relatively higher count rate advantage for a fast neutron detector. In this paper it has been shown that modern SiPMs can be used with organic scintillators for the detection of fast neutrons in the field of radiation protection applications and safety of nuclear facilities. This study demonstrated that the sensor SiPM3325-WB is the most favorable for the detection of fast neutrons if the intensity of mixed radiation is very high because it is the fastest, but if the intensity of radiation is low and the maximum count rate is not important, then the sensor MicroFC-60035-SMT is better because of its higher gain and a larger photosensitive area (see table 1) which allows it to have a relatively greater detection efficiency.

References

[1] https://www.sciencedirect.com/topics/earth-and-planetary-sciences/proportional-counter
[2] Liao C and Yang H 2015 Pulse shape discrimination using EJ-299-33 plastic scintillator coupled with a silicon photomultiplier array *Nucl. Instrum. Methods. Phys. Res. A* **789** 150–7
[3] Prettyman T H 2014 *Encyclopedia of the Solar System (Third Edition)* ed T Spohn *et al* (Elsevier) pp 1161–83
[4] Birks J B 1964 *Theory and Practice of Scintillation Counting* ed D W Fry *et al* (New York: Pergamon Press)
[5] Lee S K, Kang B H, Kim G D and Kim Y K 2012 Performance improvement of neutron flux monitor at KSTAR *J. Instrum.* **7** 6
[6] https://www.inradoptics.com/pdfs/datasheets/InradOptics_Datasheet_Stilbene
[7] Zaitseva N, Glenn A, Carman L, Hatarik R, Hamel S, Faust M, Schabes B, Cherepy N and Payne S 2011 Pulse shape discrimination in impure and mixed single-crystal organic scintillators *IEEE Trans. Nucl. Sci.* **58** 3411–20
[8] https://www.hamamatsu.com/resources/pdf/etd/PMT_handbook_v3aE.pdf
[9] https://www.hamamatsu.com/resources/pdf/ssd/e03_handbook_si_apd_mppc.pdf
[10] Vinogradov S and Popova E 2020 Status and perspectives of solid state photon detectors *Nucl. Instrum. Methods. Phys. Res. A* **952** 161752
[11] Preston R M, Eberhardt J E and Tickner J R 2014 Neutron-gamma pulse shape discrimination using organic scintillators with silicon photomultiplier readout *IEEE Trans. Nucl. Sci.* **61** 2410–18
[12] https://www.ketek.net/wp-content/uploads/2018/12/KETEK-PM3325-WB-D0-Datasheet.pdf
[13] http://sensl.com/products/j-series/
[14] Sæterstøl J 2010 *Characterization of Scintillation Crystals for Positron Emission Tomography* (Bergen, University of Bergen) p 26
[15] Weinstock L S 2014 *Development of Front-end Electronics for Detectors with SiPM Readout* (Aachen, RWTH Aachen University)
[16] Pleshko A D, Buzhan P Z, Ilyin A L, Popova E V, Stifutkin A A and Ageev S I 2013 Studying voltage recovery processes on silicon photomultipliers *Instrum. Exp. Tech.* **56** 697–705
[17] Bychkova O V, Ilyin A L, Kayumov F F, Parygin P P, Philippov D E, Popova E V, Stifutkin A A and Vinogradov S L 2019 Study of the SiPM double component recovery time *J. Phys.: Conf. Series* **1390** 012108
[18] Brooks F D, Pringle R W and Funt B L 1960 Pulse shape discrimination in a plastic scintillator *IRE Trans. Nucl. Sci.* **7** 35–8
[19] Kim H D, Cho G S and Kim H J 2013 Characteristics of a stilbene scintillation crystal in a neutron spectrometer *Radiat. Meas.* **58** 133–7
[20] Ruch M L, Flaska M and Pozzi S A 2015 Pulse shape discrimination performance of stilbene coupled to low-noise silicon photomultipliers *Nucl. Instrum. Methods. Phys. Res. A* **793** 1–5
[21] Kim C, Yeom J Y and Kim G 2019 Digital n-γ pulse shape discrimination in organic scintillators with a high-speed digitizer *J. Radiat. Prot. Res.* **44** 53–63